www.czasopisma.pan.pl PAN POLSKA AKADEMIA NAUK www.journals.pan.pl

Arch. Metall. Mater. **66** (2021), 2, 637-643

DOI: 10.24425/amm.2021.135901

M. ŚLĘZAK[1], M. KARBOWNICZEK[1*], P. MIGAS[1], W. ŚLĘZAK[1]

HIGH TEMPERATURE STUDY OF INDUSTRIAL SLAG FROM FURTHER MODELLING POINT OF VIEW

This paper deals with the subject of high temperature analysis of refining slags originating from a ladle from an actual/industrial secondary refining process. The objective of the conducted research was to learn about the rheological behaviour of the complex industrial slag systems analysed in conditions of variable rheological parameters and temperature, also analyses with a high-temperature microscope. The analysed system seems to be a Newtonian body (with viscosity between 0.1 and 0.8 Pa·s, depend on temperature value, and chemical composition).

Keywords: viscosity, slag, steelmaking modelling

1. Introduction

The main steelmaking processes are composed of two phases – liquid steel and liquid slag. The role of slag in these processes is very important, as the manufacturing effectiveness subject to the type of steel made, the steelmaking process applied, and the process stage. A lot of paper treated about the most important functions of the steelmaking slag. From many years the scientists analysed the properties of metallurgical slags, including the changes of viscosity, which depend on temperature and chemical composition changes [1,2].

What is more, the proper chemical composition of steelmaking slags, depending on their purpose and the assigned function at a specific process stage, and on the type and grade of the steel manufactured, differ in their compositions and properties (basicity, melting temperature, viscosity, density, surface tension and interfacial tension, thermal conductivity, reactivity). Apart from purpose, viscosity is a fundamental physical parameter of slags. The metal bath desulphurisation rate, and flow rates of oxygen, hydrogen and nitrogen from the atmosphere through the slag to the liquid metal are all dependent on viscosity.

The steelmaking slag viscosity mostly is treated as a function of chemical composition, depends mainly on the SiO_2 content [3]. More silica in the slag may cause separation and entrapment of slag particles into the metal volume during stirring with inert gases, thus increasing the amount of oxide non-metallic inclusions in the metal [4,5]. However, scientists also analysed another chemical components which affect on viscosity values, such as Al_2O_3 [5,6], MgO [3], basicity [3,7]. Moreover, slags are complicated oxide systems, which due to their internal structure may feature/show non-ideal behaviour. In the literature the structure of oxide slag systems is widely analysed [7].

On the other hand, one such case is the analysis of rheological behaviour of systems that for many years used to be considered Newtonian bodies (for which viscosity is a physical parameter depending on temperature and pressure) and now are a focus of interest of many scientists [1-7]. The most often applied slags consist of: 45 ÷ 55% CaO, 35 ÷ 45% Al_2O_3, up to 10% SiO_2, and up to 1% FeO. In this paper the analysed slag systems are quite different, because they are using during ribbed bar productions. Thus the chemical composition of the applied oxide systems are a slightly changed. In this case the amount of alumina-oxides is ten times less and the percentage of silica-oxides are higher – up to 36%.

From the modelling and optimising processes point of view it is crucial to understand and analyse the rheological characteristic of slag systems [3,9,10]. These allow formulate models – equations [8] to compute value of the dynamic viscosity coefficient of different slag systems. These developed models will contain different parameters such as: chemical composition, forces impacting on the system – rheological parameter, and temperature value.

[1] AGH UNIVERSITY OF SCIENCE AND TECHNOLOGY, AL. A. MICKIEWICZA 30, 30-059 KRAKOW, POLAND

* Corresponding author: mkarbow@agh.edu.pl

2. Experimental procedure

The slags used for the tests came from an industrial process. These are refining slags formed in the ladle after tapping the steel from the arc furnace in the case of deoxidation with FeSi. The chemical composition of the formed slags is the result of adding to the ladle lime, MgO and desulphurising mix, as well as FeSi as a deoxidizer.

In this study, the following four slag systems were examined (Table 1).

TABLE 1

Chemical compositions of analyzed slag systems [%]

Sample	MgO	Al_2O_3	SiO_2	P_2O_5	S	CaO	MnO	Fe	Cr_2O_3	TiO_2
A	7,1	3,28	33,1	0,05	0,83	54,5	0,26	0,33	0,31	0,24
B	7,1	5,2	36,5	0,05	0,31	47,7	1,64	0,82	0,34	0,34
C	13,2	5,7	28,8	0,04	1,09	50,1	0,24	0,24	0,32	0,27
D	5,9	3,9	31,5	0,04	1,25	56,4	0,25	0,19	0,31	0,26

A Hesse Instruments EM 201-17/K high-temperature microscope was applied to determine the melting temperatures of the slags. Slag samples were ground, and subsequently the cylinders were formed with a diameter and a height of 3 mm. The samples were placed on graphite pads. The measurement was conducted in the argon atmosphere. Table 2 presents the applied heating diagram. Table 3 presents a comparison of the temperatures at which the sample was deformed and a "sphere" start formed.

TABLE 2

Heating diagram

Segm.	Heating rate	End temperature
1	80°C/min	800°C
2	30°C/min	1200°C
3	10°C/min	1750°C

TABLE 3

Results of experiments performed at the high-temperature microscope

Sample	Deformation point	Sphere formation
A	1248°C	1325°C
B	1261°C	1276°C
C	1250°C	1440°C
D	1188°C	1350°C

Fig. 1 presents pictures of the samples from a high-temperature microscope. In each line there is a picture of a given sample showing its appearance (starting from the left):

- before starting the measurement (turning the furnace on),
- after deformation (deformation point),
- after obtaining the "sphere".

By analysing the pictures presented in Fig. 1 and the findings in Table 3, we find that sample D deformed first (at a temperature 60°C lower than the subsequent sample), followed by sample A, sample C and sample B. The deformation of samples A and C occurred at a temperature of about 1250°C. A regular sphere was only obtained for sample B, which was characterised by the highest FeO and MnO content, while sample A had the highest SiO_2 content and the lowest Al_2O_3 content. However, sample D had the lowest FeO and MnO content, and sample C had the lowest SiO_2 content and the highest Al_2O_3 content. Therefore, we can conclude that as the FeO, MnO and SiO_2 contents increase, the temperature of sample deformation decreases. However, an increase in the Al_2O_3 content contributes to an increase in the deformation temperature.

Then the rheological tests were conducted with a FRS1600 high-temperature rheometer (details are described in [11]). The tests were conducted for three temperatures: 1520, 1510 and 1500°C and three different values of shear rate in each of temperature were applied: 15 s^{-1}, 100 s^{-1}, 10-100 s^{-1}, 100-10 s^{-1}. Taking into account the results obtained from the high temperature microscope we can assume that all of examined slag systems were liquid in this temperature range. Each of measurement was conducted during 300 s (5 minute), it was time needed for stabilizing the viscosity coefficient values. Between temperature: 1520-1510°C and 1510-1500°C the shear rate 10 s^{-1} were applied and changes of the viscosity values during cooling were measured (cooling rate was 0.3°C/min).

Figure 2 presents a graph of changes in the dynamic viscosity coefficient value of examined slag systems for constant shear rate 15 s^{-1} in a temperature 1520°C.

Analysis of curves of changes in the dynamic viscosity coefficient over time presented in Fig. 2 allows us to find that a period of about 5 minutes was needed for the value of the dynamic viscosity coefficient to stabilise. The highest values of dynamic viscosity coefficient, after 300 s (5 minutes), for the applied shear rate of 15 s^{-1} were obtained for sample D (about 0.5 Pa·s), and next for sample C (about 0.3 Pa·s), A (0.2 Pas) and B (0.18 Pa·s). The curves for sample B and A partially coincided.

Figure 3 presents a graph of changes in the dynamic viscosity coefficient value of examined slag systems for constant shear rate 100 s^{-1} in a temperature 1520°C.

The curves presented in Figure 3, showing the change in the value of the dynamic viscosity coefficient of the ladle slags tested for the applied shear rate of 100 s^{-1} are contained in a much narrower range (in terms of diversification of the values of the dynamic viscosity coefficient) than for graphs presented in Figure 2. The highest values of dynamic viscosity coefficient were obtained for sample C (0.27 Pa·s), followed by sample D (0.23 Pa·s), sample B (0.22 Pa·s) and sample A (0.18 Pa·s).

Figures 4a and 4b present the changes in the values of dynamic viscosity coefficients of the slag systems tested, subject to changes in shear rate values at a temperature of 1520°C. The shear rate was changed in two steps: the shear rate change from 10 to 100 s^{-1} in 300 s, and from 100 to 10 s^{-1} in 300 s. The above described measurement diagram was applied to verify changes in the values of dynamic viscosity coefficient with reference to the thixotropy effect, related to the formation and disintegration of particle agglomerates.

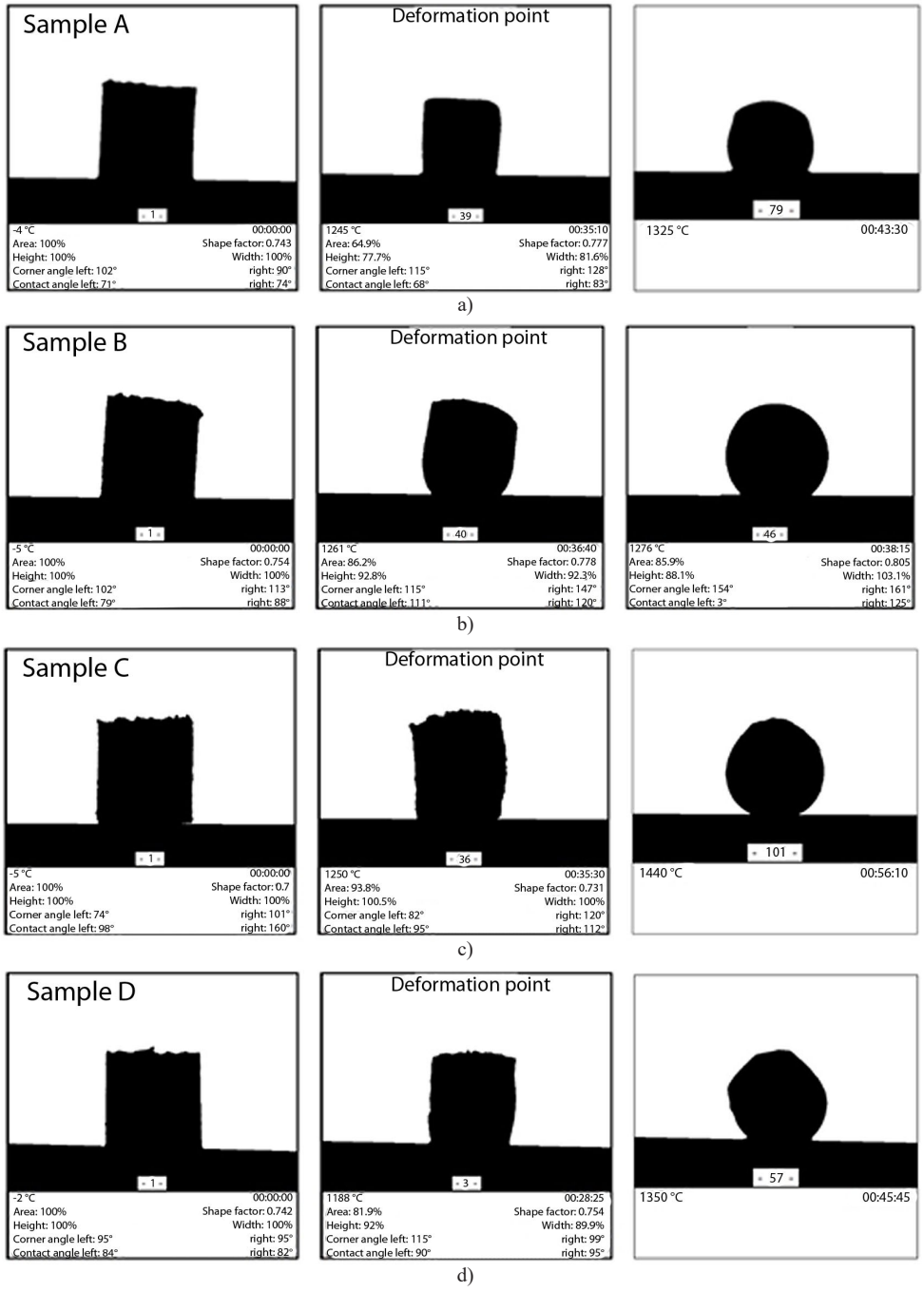

Fig. 1. Pictures of the samples from a high-temperature microscope a) sample A b) sample B c) sample C d) sample D

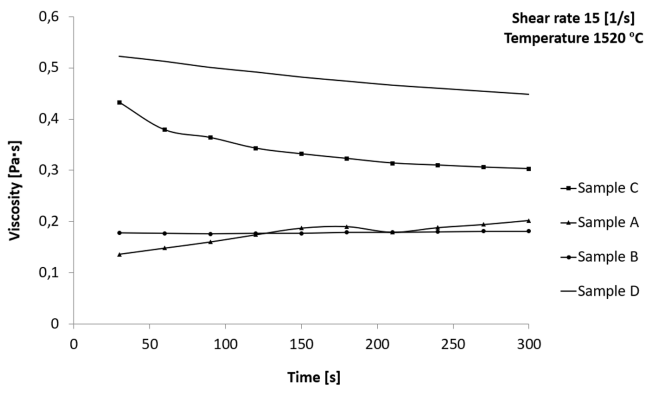

Fig. 2. Changes in the dynamic viscosity coefficient values of analysed slag systems in time for constant shear rate value

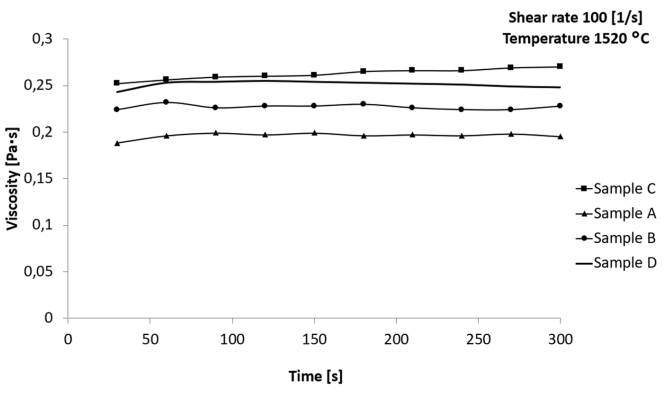

Fig. 3. Changes in the dynamic viscosity coefficient values of analysed slag systems in time for constant shear rate value

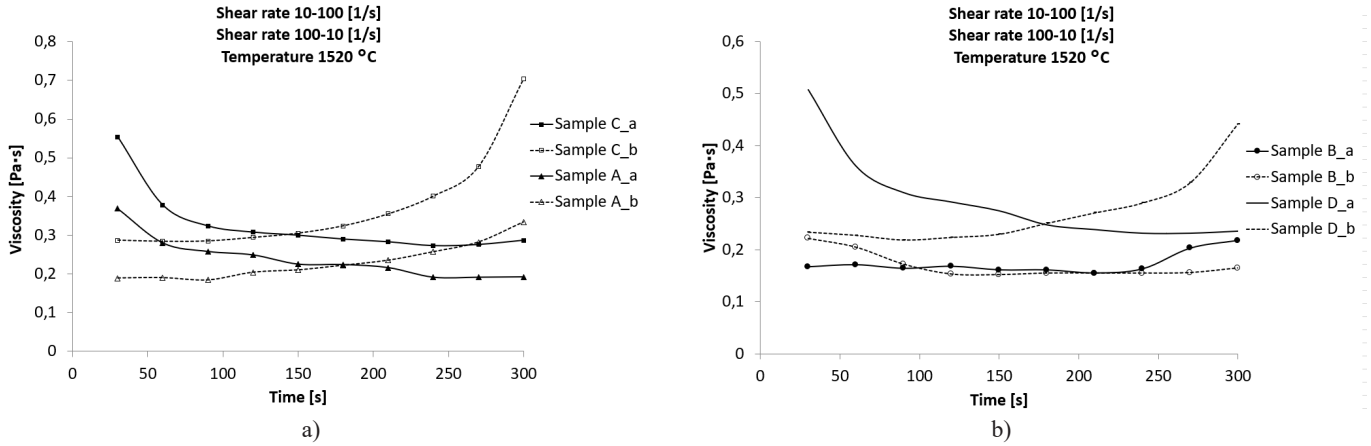

Fig. 4. Changes in the dynamic viscosity coefficient values of analysed slag systems in time for changeable shear rate values 10-100 s^{-1} and 100-10 s^{-1} for a) sample A and C; b) sample B and D

For each of the analysed slags, we observed that the dynamic viscosity coefficient value declined as the shear rate increased (10-100 s^{-1}). At the same time, when the shear rate decreased again (100-10s^{-1}) the values of the dynamic viscosity coefficient of the slag systems tested grew again, reaching values similar to the "previous" ones (obtained for the analogous values of shear rate in step a). Therefore, viscosity curves do not form hysteresis loops, which, among others, are characteristic to suspensions. As in the previous cases (results presented in Fig. 2 and 3) the highest values of dynamic viscosity coefficient were obtained for sample C, followed by sample D, sample A, sample B. For samples A and B, the values of dynamic viscosity coefficients fluctuate, i.e. the lowest (out of the four systems tested at a temperature of 1520°C) values of the viscosity coefficient (15 s^{-1}) were obtained once for sample B, another time (100 s^{-1}) for sample A. The difference in the values of the dynamic viscosity coefficient was ca. 0.02 Pa·s.

Fig. 5 presents a graph of changes in the dynamic viscosity coefficient values of the slag systems analysed over 30 minutes (1800 s), when the temperature changed from 1520°C to 1510°C.

On the basis of the analysis of the graphs presented in Fig. 5, we can find that for three of the slag systems analysed (samples D, A, B), over 30 minutes the dynamic viscosity coefficient increases as the temperature decreases. For sample C, an increase in the values of the dynamic viscosity coefficient as the temperature decreased were not observed; however during further tests performed at a temperature of 1510°C, presented hereinafter, it was found that the dynamic viscosity coefficient value of sample C increased (compared to the temperature of 1520°C).

Fig. 6 presents a graph of changes in the dynamic viscosity coefficient value of examined slag systems for constant shear rate 15 s^{-1} in a temperature 1510°C.

The analysis of changes in the values of the dynamic viscosity coefficient over time presented in Fig. 6 allows us to find that the highest values of dynamic viscosity coefficient, after 300 s (5 minutes), for an applied shear rate of 15 s^{-1} were obtained for sample C (about 0.55 Pa·s), and followed by sample D (about 0.38 Pa·s), sample A (0.32 Pa·s), and sample B (0.19 Pa·s). The order of samples in terms of their dynamic viscosity coefficients was similar to the order obtained at a temperature of 1520°C; however at that point the highest value of dynamic viscosity coefficient was obtained for sample D, followed by sample C. At the same time, we can find that the values of dynamic viscosity coefficient increased for all slag systems analysed when the temperature dropped by 10°C.

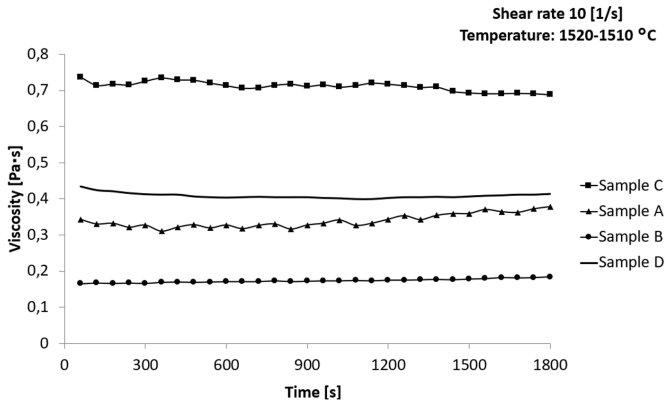

Fig. 5. Changes in the dynamic viscosity coefficient values of examined slag systems during cooling

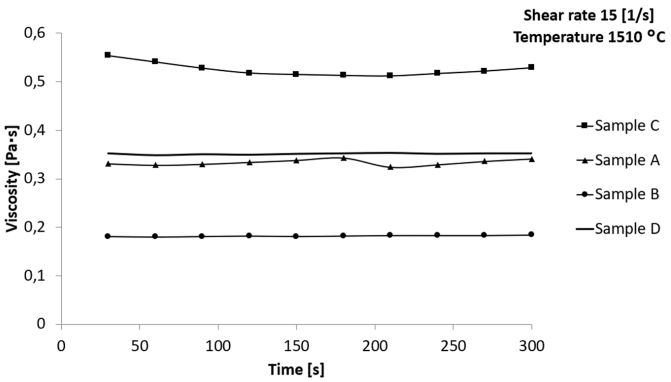

Fig. 6. Changes in the dynamic viscosity coefficient values of analysed slag systems in time for constant shear rate value

Figure 7 presents a graph of changes in the dynamic viscosity coefficient value of examined slag systems for constant shear rate 100 s^{-1} in a temperature 1510°C .

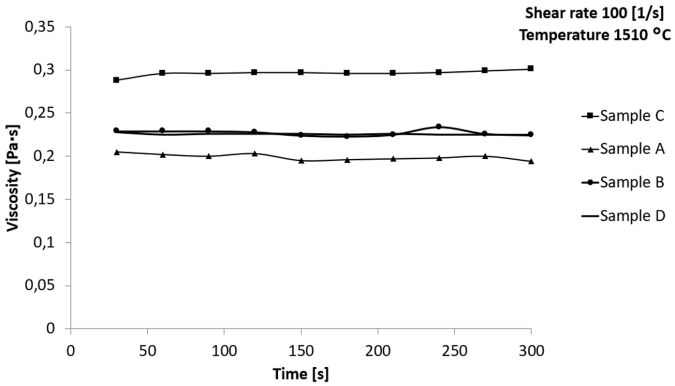

Fig. 7. Changes in the dynamic viscosity coefficient values of analysed slag systems in time for constant shear rate value

The curves presented in Fig. 7 showing the change in the value of the dynamic viscosity coefficient of the ladle slags tested for an applied shear rate of 100 s^{-1} are contained in a much narrower range (in terms of the diversification of the values of the dynamic viscosity coefficient) than the graphs presented in Figure 6 (analogous as for results presented in Fig. 2 and Fig. 3). The highest values of dynamic viscosity coefficient were obtained for sample C (0.30 Pa·s), followed by sample D and sample B (0.24 Pa·s), and sample A (0.20 Pa·s). The order of samples in terms of their dynamic viscosity coefficients was similar to the order obtained at a temperature of 1520°C, however at that point the values of the dynamic viscosity coefficient obtained for sample D and sample B were not the same (the value of dynamic viscosity coefficient for sample D was higher by 0.01 Pa·s). At the same time, we can observe that as the temperature dropped by 10°C, the values of the dynamic viscosity coefficient increased for all slag systems analysed, for an applied shear rate of 100 s^{-1}.

Figures 8a and 8b present the changes in the values of dynamic viscosity coefficients of the slag systems tested, subject to changes in shear rate values at a temperature of 1510°C. The shear rate was changed in two steps: the shear rate change from 10 to 100 s^{-1} in 300 s, and from 100 to 10 s^{-1} in 300 s. The above described measurement diagram was applied to verify changes in the values of dynamic viscosity coefficient with reference to the thixotropy effect, related to the formation and disintegration of particle agglomerates.

For each of the slags analysed, we can observe that the dynamic viscosity coefficient value declines as the shear rate increases (10-100 s^{-1}). At the same time, when the shear rate decreases once again (100-10 s^{-1}), the values of the dynamic viscosity coefficient of the slag systems tested grow again, reaching values similar to the "previous" ones (obtained for the analogous values of shear rate in step a). The viscosity curves do not form a hysteresis loop, they coincide. As in the previous cases concerning the temperature of 1520°C, the measurement was conducted in an analogous regime the highest values of the dynamic viscosity coefficient were obtained for sample C, followed by sample D, sample A, sample B.

Fig. 9 presents a graph of changes in the dynamic viscosity coefficient values of the slag systems analysed over 30 minutes (1800 s), when the temperature changed from 1510°C to 1500°C. We can find that for all the slag systems analysed the dynamic viscosity coefficient increases over 30 minutes as the temperature decreases by 10°C.

Fig. 10 presents a graph of changes in the dynamic viscosity coefficient value of examined slag systems for constant shear rate 15 s^{-1} in a temperature 1500°C. We can find that the highest values of dynamic viscosity coefficient, after 300 s (5 minutes), for an applied shear rate of 15 s^{-1} were obtained for sample C (about 0.80 Pa·s), followed by sample D (about 0.40 Pa·s), sample A (0.38 Pa·s), and sample B (0.20 Pa·s). The order of samples according to the dynamic viscosity coefficient values is similar to the order obtained at temperatures of 1520°C and 1510°C. At the same time, we can find that the highest increase in the dynamic viscosity coefficient, at a temperature change of 10°C and at the same measurement regime (Fig. 6), was for sample C (from 0.55 to 0.80 Pa·s). However, the lowest increase in the dynamic viscosity coefficient was for sample B (from 0.19 to 0.20 Pa·s).

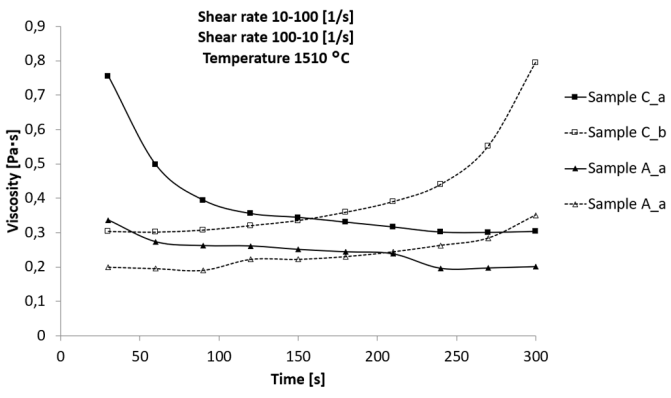

a)

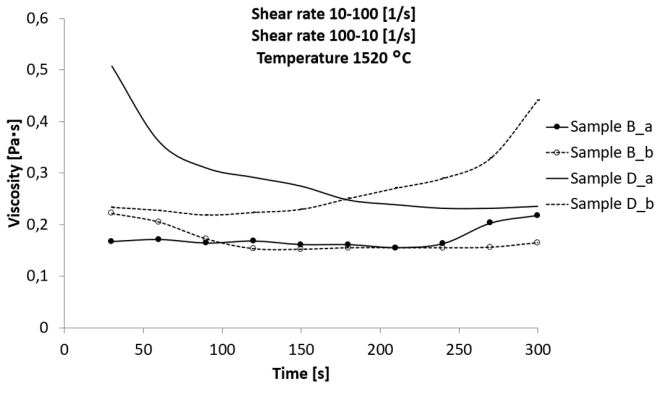

b)

Fig. 8. Changes in the dynamic viscosity coefficient values of analysed slag systems in time for changeable shear rate values 10-100 s^{-1} and 100-10 s^{-1} for a) sample A and C; b) sample B and D

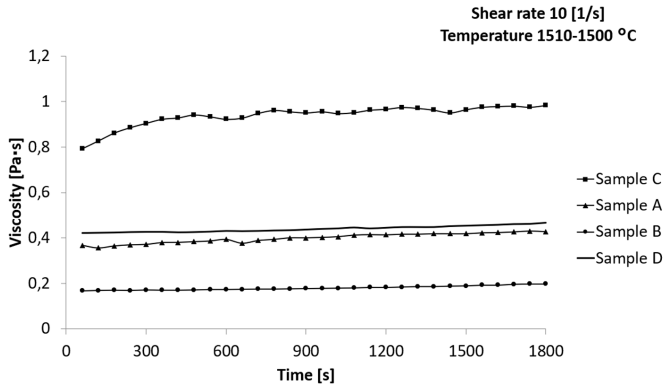

Fig. 9. Changes in the dynamic viscosity coefficient values of examined slag systems during cooling

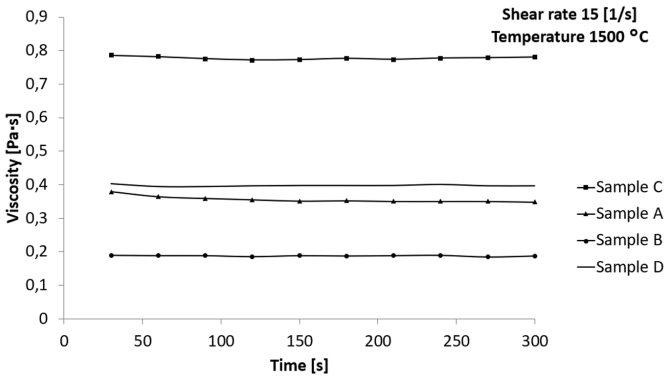

Fig. 10. Changes in the dynamic viscosity coefficient values of analysed slag systems in time for constant shear rate value

Fig. 11 presents a graph of changes in the dynamic viscosity coefficient value of examined slag systems for constant shear rate 100 s^{-1} in a temperature 1500°C. The presented curves for an applied shear rate of 100 s^{-1} are contained in a much narrower range (in terms of the diversification of the values of the dynamic viscosity coefficient) than for the graphs presented in Fig. 9 (analogous as for results presented in Fig. 2 and Fig. 3, as well as Fig. 6 and Fig. 7.) The highest values of dynamic viscosity coefficient were obtained for sample C (0.33 Pa·s), followed by sample D (0.25 Pa·s), sample B (0.245 Pa·s) and sample A (0.23 Pa·s). The order of samples according to the dynamic viscosity coefficient values is similar to the order obtained at a temperature of 1510°C. At the same time, we can find that as the temperature dropped by 10°C (compared to findings shown in Fig. 7), the values of the dynamic viscosity coefficient increased for all slag systems analysed, for an applied shear rate of 100 s^{-1}.

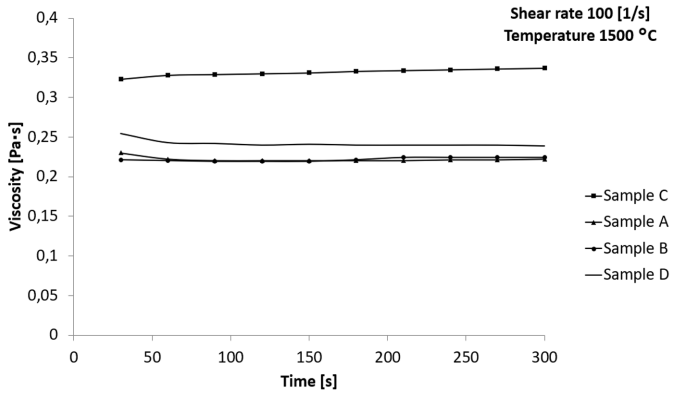

Fig. 11. Changes in the dynamic viscosity coefficient values of analysed slag systems in time for constant shear rate value

Figures 12a and 12b present the changes in the values of dynamic viscosity coefficients of the slag systems tested, subject to changes in shear rate values at a temperature of 1500°C. The shear rate was changed in two steps: the shear rate change from 10 to 100 s^{-1} in 300 s, and from 100 to 10 s^{-1} in 300 s. The above described measurement diagram was applied to verify changes in the values of dynamic viscosity coefficient with reference to the thixotropy effect, related to the formation and disintegration of particle agglomerates.

For each of the slag systems investigated, we can observe that the dynamic viscosity coefficient value declines as shear rate increases (10-100 s^{-1}). At the same time, when the shear rate decreases once again (100-10 s^{-1}), the values of the dynamic viscosity coefficient of the slag systems tested grow again, reaching values similar to the "previous" ones (obtained for the analogous

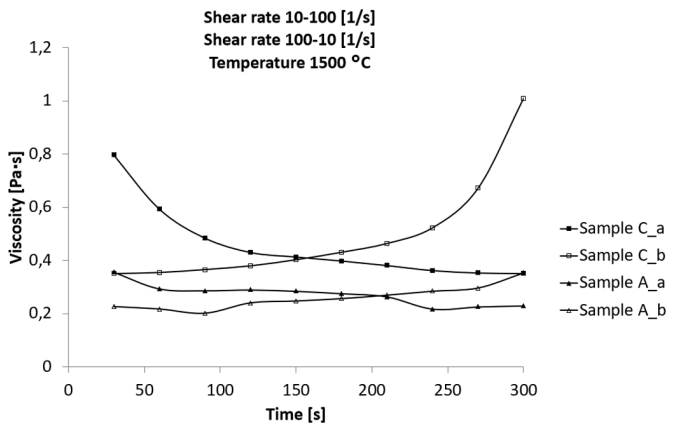

a)

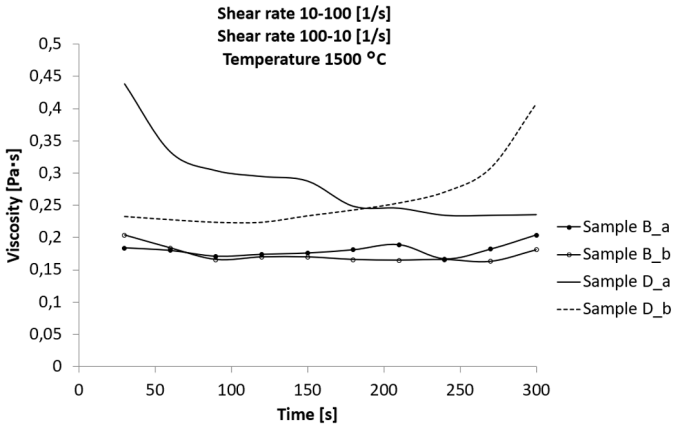

b)

Fig. 12. Changes in the dynamic viscosity coefficient values of analysed slag systems in time for changeable shear rate values 10-100 s^{-1} and 100-10 s^{-1} for a) sample A and C; b) sample B and D

values of shear rate in step a). The viscosity curves do not form a hysteresis loop, they coincide. The highest values of dynamic viscosity coefficient were obtained for sample C, followed by sample D, sample A, sample B.

In addition, based on the conducted rheological analysis, we can say that higher dynamic viscosity coefficients of the slag systems analysed were obtained at lower shear rates (10 s^{-1}, 15 s^{-1}), while lower dynamic viscosity coefficients were obtained at higher shear rates (100 s^{-1}). Furthermore, the range (dispersion of values on the Y axis) of values of the dynamic viscosity coefficient was smaller when higher shear rates were applied.

The systems analysed did not show the thixotropy effect. However, an increase in the viscosity coefficient was observed when the shear rate was changed "in one direction" – i.e. 10-100 s^{-1}, and there was a decline in this value when the shear rate was changed 100-10 s^{-1}. However these curves coincided, thus not forming a hysteresis loop.

The highest values of the dynamic viscosity coefficient (with small deviations, e.g. at 1520°C, and a shear rate of 15 s^{-1}), at each of the applied temperatures, with various measurement regimes, were observed in the following order: C, D, A, B. So, looking from the lowest values of dynamic viscosity coefficient, the order was as follows: sample B, sample A, sample D, sample C. An analogous order was obtained from tests performed with a high-temperature microscope with regard to the temperature at which the "sphere" formed (from the lowest temperature the order was as follows: B, A, D, C).

In addition, for all slag systems tested, an increase in the dynamic viscosity coefficient was observed as the temperature decreased, and the biggest increase in the dynamic viscosity coefficient when the temperature changed by 20°C was observed for sample C (for this system generally the highest values of dynamic viscosity coefficient were observed). On the other hand, the smallest differences in values of dynamic viscosity coefficient, when the temperature change was 20°C, were observed for sample B.

3. Conclusions

- Based on the results of measurements performed with a high-temperature rheometer, it was found that the "sphere" was formed by the slag systems analysed in the following order: sample B, sample A, sample D, sample C.
  At the same time, it was found that a regular sphere was only formed for sample B, which contained the most FeO and MnO of the samples tested.
- Based on the results of rheological measurements, it was found that the values of dynamic viscosity coefficient, in ascending order, were as follows: sample B, sample A, sample D, sample C.
  Sample B featured the highest FeO and MnO content; sample A the highest SiO_2 content and the lowest Al_2O_3 content; sample D the lowest FeO and MnO content; sample C the lowest SiO_2 content and the highest Al_2O_3 content.
  Therefore, we can conclude that as the FeO, MnO and SiO_2 contents increase, the temperature of sample deformation decreases, and the values of the dynamic viscosity coefficient decline. However, an increase in the Al_2O_3 content favours an increase in the deformation temperature and beings about an increase in the dynamic viscosity coefficient.
- It was observed that the dynamic viscosity coefficient grew as the temperature decreased.
- The values of the dynamic viscosity coefficient of the slag systems analysed differed subject to the applied shear rates (15 s^{-1}, 100 s^{-1}, 10-100 s^{-1}, 100-10 s^{-1}). At the same time, the results of tests performed with the high-temperature microscope allowed us to state that all of the systems tested, at the temperatures analysed (1520°C, 1510°C, 1500°C), were in the fully liquid state. Therefore, the non-Newtonian nature of the flow of the systems tested resulted from the presence of solids in the slag systems.

Aknowledgements

Research financed through subvention funds of AGH University of Science and Technology in Krakow, no. 16.16.110.663/6.

REFERENCES

[1] A. Chychko, S. Seetharaman, Metall. Mater. Trans. B **42**, 20-29 (2011).
[2] E.B. Pretorius, R.C. Carlisle, Proceedings of the 56th Electric furnace conference 275-292 (New Orleans, LA, USA, 1998).
[3] T. Talapaneni, N. Yedla, S. Pal, S. Sarkar, Metall. Mater. Trans. B, **48**, 1450-1462 (2017).
[4] L. Holappa, Treatise on Process Metallurgy **3**, 301-43 (2014): Industrial Processes, Elsevier, Oxford.
[5] V.C. Da Rocha, J.A.M. Pereira, A. Yoshioka, W.V. Bielefeldt, A.C.F. Vilela, Metall. Mater. Trans. B **48**, 1423-1432 (2017).
[6] Y. Sasaki, H. Urata M. Iguchi, M. Hino, ISIJ Int. **46**, 385-87 (2006).
[7] T. Wu, Q. Wang, C. Yu, S. He, J. Non-Cryst. Solids **450**, 23-31 (2016).
[8] M. Ślęzak, Arch. Metall. Mater. **60**, 581-589 (2015).
[9] K. Sunahara, K. Nakano, M. Hoshi, T. Inada, S. Komatsu, T. Yamamot, ISIJ Int. **48**, 420-29 (2008).
[10] G.-H. Zhang, K.-C. Chou, K. Mills, Metall. Mater. Trans. B, **45** 698-706 (2014).
[11] M. Korolczuk-Hejnak, P. Migas, Arch. Metall. Mater. **57**, 963-969 (2012).